ISMSSE 2018

Check for updates

Research on the effect of coal seam inclination on gas migration channels at fully mechanized coal mining face

Pengxiang Zhao[1,2] · Risheng Zhuo[1] (iD) · Shugang Li[1,2] · Chun-Hsing Ho[3] · Haifei Lin[1,2] · Hui Liu[1]

Abstract

To investigate the mechanical evolution progress of mining-induced pressure-relief gas migration channel in overlying strata fissure at fully mechanized mining working face, physical similarity simulation tests were conducted to experimentally and numerically evaluate the mining process of a coal mine in Heshun, Shanxi Province. The profiles of the gas migration channels were mathematically modeled based on the theory of elliptical zone of mining-induced fissure, using the dip angle of coal seams of working face as the key parameter. The impacts of dip angle of coal seams on the evolution of pressure-relief gas migration channel in overlying strata fissure at the main mining working face were analyzed. Results suggested that the increase in the dip angles of coal seams could reduce the height of the three zones and could expand the average weighting interval; the gas migration channels were formed at lower positions in the overlying strata, resulting in the lower height, width, caving angle, and range; in addition, with the increase of the dip angle, the segregation and propagation rates of the gas migration channel gradually increased, and the fractal dimensions of coal seams are measured in between 1.68, 1.69, and 1.71, displaying an increasing trend. On-site high-level boreholes were arranged to validate the laboratory results. Based on the monitoring, the gas extraction through the high-level borehole field reached 49.94~89.88% of the total gas emission. In general, the average concentration of gas in the upper corner is maintained below 0.27% and the average concentration of gas in the return airway is maintained below 0.32% so as to ensure a safe and an efficient mining environment. The study contributes to the theoretical basis for identification of pressure-relief gas enrichment areas in overlying strata under the effect of dip angle of coal seams.

Keywords Mining-induced overlying strata fissure · Gas migration channels · Angle of coal seams · Mining working face · High-level boreholes

Introduction

China has large coal reserves, which leads to one of the biggest production and consumption of coal in the world. Coal accounts for 77% and 66%, respectively, in production and consumption of primary energy (Yuan 2016, 2017). With the rapid development of China's economy, the demand on coal production has been increasing continuously. However, the ever-increasing mining intensity has resulted in significant increased gas relief and increased occurrence of gas overrunning and correspondingly gas explosion (Xie et al. 2017; Li et al. 2014a, b; Wu et al. 2018a, b), which has been severely compromising both safety and efficiency of coal mines. In the past years, many efforts have been devoted to analyzing the evolution of mining-induced overlying strata fissure and migration patterns of pressure-relief gas, particularly with focus on the impacts of the features of coal seam, conditions of mining working face, and geological structures on the progress of mining-induced overlying strata fissure network configurations (Do et al. 2017; Palchik 2015; Li et al.

✉ Risheng Zhuo
zhuorisheng@163.com

1   School of Safety Science and Engineering, Xi'an University of Science and Technology, Xi'an 710054, Shaanxi, China

2   Key Laboratory of Western Mine Exploitation and Hazard Prevention with Ministry of Education, Xi'an 710054, Shaanxi, China

3   Department of Civil Engineering, Northern Arizona University, Flagstaff, AZ 86011, USA

2018a, b; Pan et al. 2014; Zhang et al. 2015; Wu et al. 2018a, b; Gu et al. 2018; Zhang et al. 2018a, b). For example, Qian and Miao (1996) and Liu (1995) proposed the three horizontal zones and three vertical zone theory and the O-shaped circle theory are used in the emergence of additional knowledge and theories. Xue et al. (2014); Guo and Yuan (2015), Zhang et al. (2018a, b), and Liu et al. (2015) proposed the theory of annular fracture ring of the coal seam roof and the double-circle theory to evaluate the evolution of mining-induced cracks. Zhang et al. (2018a) further conducted a series of physical and mathematical simulations to compare the results with the above theories. In addition, Li et al. (2014a, b, 2016, 2017) proposed the elliptic-paraboloid zone of mining-induced fissure theory and established an engineering simplified model of mining-induced fissure round-rectangle trapezoidal zone based on data from the mining site.

The researches of the scholars mentioned above are mainly focused on the coal seams near the ground level. However, the crack propagations of the overlying strata of inclined coal seams have numerous differences compared with the horizontal coal seams. Therefore, in response to this problem, many scholars have conducted experiments and extensive researches on the fracture evolutions of deep coal seams. Wang et al. (2015, 2018), Lai (2015); Shan and Lai (2018), and other scholars established a spatial model of the "key layer" rock mass structure with longwall mining in large dip angles under asymmetrical constraint conditions, inclined angles, and vaulted coal rocks. The destabilization caused the partial pressure distortion on the working face and induced dynamic disasters to be elaborated. Guo (2016) and Zhang and Gao (2016) studied the dredging patterns of overlying strata on the working face of steeply inclined medium-thick coal seams. Their work was based on field observations and theoretical analysis using the "semicircular arch" structural mechanics model. Sun (2018) studied the characteristics of bottom mining failure of the inclined face, and the result indicated that the morphological change is similar to the "spoon-shaped" distribution pattern. Zhang (2013) combined a UDEC numerical simulation to investigate the distribution of gas flow channels at different dip angles using an asymmetric "saddle"-type to "duck egg"-type distribution model.

In this paper, the physical similarity simulation test method was used to study the mechanism and evolution law of gas migration channels of overburden fissures for coal seams of a high gassy coal mine in Heshun, Shanxi Province. A mathematical model of the gas migration channel evolution of overlying strata in tilted coal seams is constructed. The objectives of the paper are to (1) provide a theoretical basis to accurately identify the gas-recovery and gas accumulation zones of overlying strata, (2) determine the indicating parameters of the gas-relief gas drainage system, and (3) improve the efficiency of pressure-relief gas drainage system.

Test design

Background of field site

The laboratory test was designed to simulate the main mining working face of a highly gassy coal mine in Heshun, Shanxi Province, where the length is 2081 m, the mining elevation is + 1150 m, the average buried depth is 410 m, and the average thickness of coal seam is 5.1 m. The average inclination angle is 7°, indicating that the mine was a flat seam. The longwall and full thickness 2 mining technologies were adopted in the working face, and the caving method was used to manage the roof. The immediate roof consisted of mudstones containing arenite in certain regions; the main roof was formed by medium sandstones and the immediate floor was formed by aluminum-rich mudstones. A model of longwall coal mining was established, and the mining heights of overlying strata

Table 1   Stimulation height of overlying strata

No.	Lithology	Thickness (m)
1	Sand mudstone	2.4
2	Aluminum mudstone	0.2
3	15# coal	5.1
4	Mudstone	0.5
5	Middle sandstone	7.1
6	Siltstone	3
77	Sand mudstone	3.7
8	114# coal	0.8
9	Siltstone	1
10	Mudstone	1.7
11	14# coal	0.8
12	K_2 limestone	5.5
13	Siltstone	2.8
14	Fine sandstone	6.1
15	Sand mudstone	2
16	13# coal	0.5
17	K_3 limestone	3
18	Sand mudstone	1
19	Fine sandstone	0.8
20	Aluminum mudstone	0.5
21	Fine sandstone	2.2
22	Sand mudstone	4.5
23	12# coal	1
24	Sand mudstone	3.4
25	Siltstone	0.9
26	11# coal	0.3
27	K_4 limestone	4.65
28	Sand mudstone	7.75
29	Fine sandstone	4
30	Sand mudstone	2.7

Table 2 Physical-mechanical parameters of coal seam

No.	Lithology	Weight (kN m^{-3})	Elastic modulus (GPa)	Compressive strength (MPa)	Poisson's ratio
1	Mudstone	20.80	20	20.5	0.195
2	Sand mudstone	26.40	56	48.8	0.278
3	Middle sandstone	26.60	50	65.1	0.280
4	Fine sandstone	26.20	43	69.0	0.260
5	Siltstone	26.00	54	58.5	0.253
6	Limestone	26.50	47	91.2	0.230
7	Aluminum mudstone	13.00	40	16.0	0.250
8	Coal	14.60	14	13.5	0.275

and the physical-mechanical parameters of coal seam were shown in Table 1 and Table 2.

Experiment design and method

The test utilized a multifunctional simulation test rig developed by the authors (Fig. 1) to build a physical model with a ratio of 1:100 to physically simulate the performance of the coal site. The coal seam direction was used as the working face recovery direction, and starting experimental study on evolution law of gas-relief pressure gas migration channel for mining overburden under the effect of different coal seam angles. Referring to the coal mine safety regulations and combining the dip of a coal seam in the field, the mining was divided into near horizontal ($< 8°$), inclined ($8°-25°$), and deeply inclined ($> 25°$) coal seams. Due to the limitations of existing laboratories, each angle of physical similarity simulations could not be carried out. Combined with the classification of coal seams, the three angles of coal seams were selected ($0°$, $15°$, and $30°$) for study in the laboratory. And in the following experiments, we will continue to make a more in-depth discussion on the gas migration law in each inclined coal seam.

According to the characteristics of physical similarity simulation, the model needs to meet similar conditions such as geometry, time, and corresponding physical quantity, so the

following settings are provided for the test: geometric similarity ratio, $a_L = 100$; similar weight ratio, $a_y = \gamma_H / \gamma_M = 1.5$; stress similarity ratio, $a_\sigma = a_L = 100$; the time similarity ratio, $a_t = \sqrt{(a_L)} = 10$. Among them, γ_H is the density of the prototype material, γ_M is the density of the model material, and a_γ is the similarity constant of the bulk density.

In the physical similarity simulation experiment, the evolution law of the gas migration channel was explored by changing the inclination angles of the coal seam ($0°$, $15°$, and $30°$). The evenly distributed load was applied on top of coal seams. The stress changes, displacements, crack propagations, and crack length changes along the surface of the specimen were recorded and measured. At the same time, the working surface was pushed and photographed which was used to analyze the development of overlying rock fissures.

Analysis of test results

Distribution characteristics of overlying strata "three zones"

As the dip angle of the coal seam increases, the height of the three zones also increases. The larger the dip angle, the more complex the force of the rock formations and the increase of
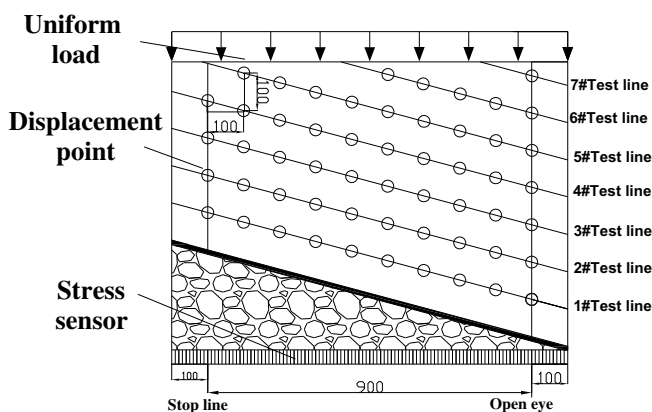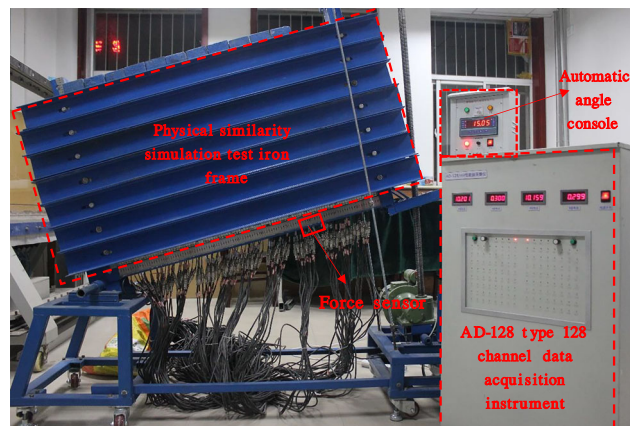

Fig. 1 Physically similar simulation test model design and test bench

the clearance space, resulting in an increase in the height of the three zones (Fig. 2).

The collapsing situations of the overburdens under different dip angles are also different. With the advancing of the working face, the rocks were getting collapsed that led to the fact that the fallen space was gradually compacted. The overlying strata formed a vertical three-segment fracture pattern in the vertical direction (the caving zone, the fractured zone, and the continuous bending zone). As the height of the fracture zone increases with the increase of the inclination angle, the area occupied by the overlying rock formation also increases, making the gas dominant and vibrant in the fracture zone. The height of the channel shows a rising trend. In the fracture area above the active area, more broken and separated cracks penetrate each other, providing relief channels for pressure-relief gas and making the height of the gas migration channel in the fracture zone.

Characteristics of pressure step variation at different coal seam angles

During the advancing process of the working face, the rock layer has fallen, and the original stress of the rock layer above the gob was released under the influence of mining, and the overlying strata gradually bent to a certain distance along the working surface until the rock strata under the lower struts cannot withstand the stress of the upper strata, causing the coal seam to collapse.

When the coal seam inclination angle was 0°, pressure occurred once every 10~15 m at the working face, with an average of 12.5 m (Table 3), which was 0.33~0.5 times greater than the initial pressure.

When the coal seam inclination angle was 15°, the working face compressed once every 7~18 m, with an average of 11.6 m (Table 4), 0.26~0.63 times greater than the initial pressure.

When the coal seam inclination angle was 30°, the pressure was generated once every 8~15 m at the working face, with an average of 10.5 m (Table 5), which was 0.23~0.43 greater than the initial pressure.

Combined with Tables 3, 4, and 5 and Fig. 3, it can be seen that with the continuous advancement of the working face, the weighting intervals are different based on different coal seam inclination angles, and the average pressure at 0° is 12.5 m, that is 1.08 and 1.19 times greater than that at 15° and 30°. In the cycle of pressure, the gas migration channel is growing quickly. With the increase of the dip angle, the average pressure step becomes smaller, and the developmental cycle of the gas migration channel is also shortened, providing more time for the slow and sufficient development of the gas migration channel.

Fig. 2 Three-zone division of the overlying rock under different dip ▶ angles. **a** Gas migration channel division diagram when the coal seam inclination angle is 0°. **b** Gas migration channel division diagram when the coal seam inclination angle is 15°. **c** Gas migration channel division diagram when the coal seam inclination angle is 30°. **d** The three zones' height variation curves of different inclination angles

Subsidence of the overlying rock layer

When the working surface is advanced to a certain distance, the overlying rock formations bend, break, and fall. The variation trend between the subsidence of overburden and the dip angle of coal seam is shown in Fig. 4.

From Fig. 4, it can be found that as the dip of the coal seam increases, the amount of subsidence of the overlying rock layer changes asymmetrically, and the amount of rock subsidence near the working face increases. In addition, the declining rock formation is influenced by the sliding effect. The collapsed rocks and blocks slide along the slope direction toward the bottom. At the same time, those fractured rocks are restrained by the rock formation in the oblique direction, reducing the falling of the rock formation above the bottom of the slope, and increasing the sagging space of rock formations in the upper part of the slope direction. As a result, the largest amount of subsidence of the rock formations near the working face was observed that led to the formation of an asymmetrical sinking curve.

For coal seams with different dip angles, the maximum subsidence is mainly concentrated on rock formations that come closer to the roof of the coal seam and the size is different. The maximum subsidence controls the severity of the collapse of the upper rock formation and the final shape of the collapse. The variation of maximum subsidence in different deep coal seams is shown in Fig. 4d. The maximum amount of subsidence is directly proportional to the dip angle of the coal seam. The maximum subsidence of the overburden increases with the increase of coal dip.

Geometry parameter distribution characteristics of gas migration channels

For different coal seam dip conditions, the height, width, and range of the gas migration channel for gas migration show different variations, as showed in Fig. 5.

It can be observed in Fig. 5 that as the mining working face advances forward, the height difference between the inner and outer boundaries of the gas migration channel increases at first and then adversely decreases. The height difference between the inner and outer boundaries at the inclination angle of 0° is "0," while the height difference between the inclination angles of 15° and 30° appeared to be gradually smaller. When the other conditions remain the same, the width of the gas migration channel at the increasing inclination angles is obviously
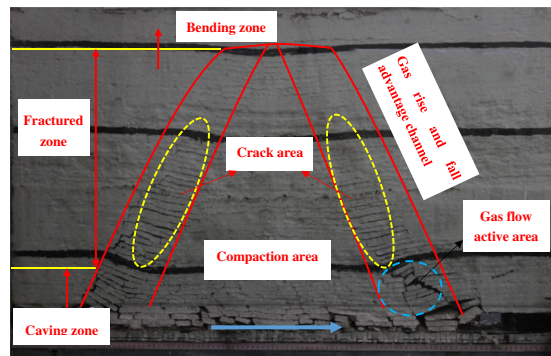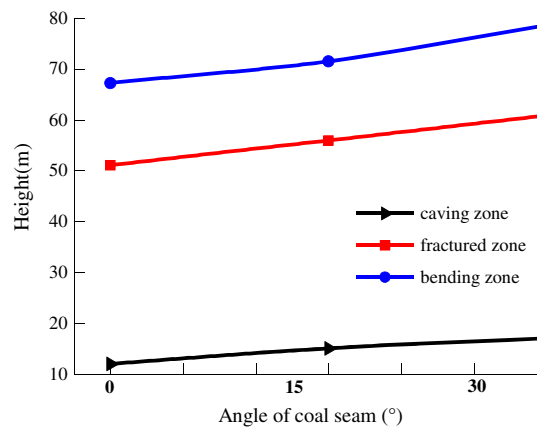
(a) Gas migration channel division diagram when the coal seam inclination angle is 0°
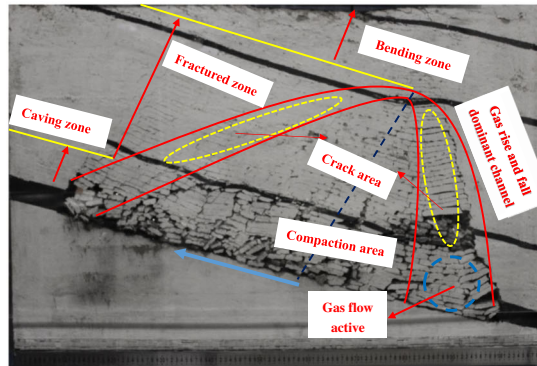
(b) Gas migration channel division diagram when the coal seam inclination angle is15°
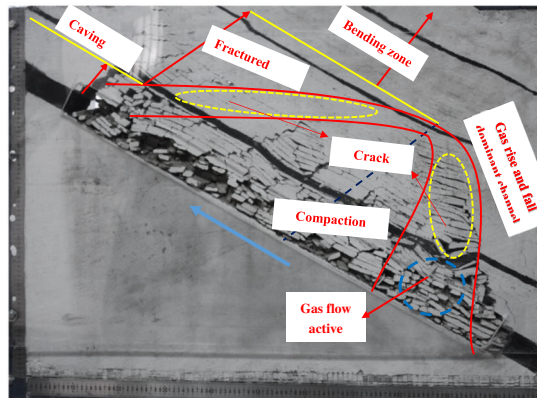
(c) Gas migration channel division diagram when the coal seam inclination angle is 30°

(d) Three zones height variation curves of different inclination angles

Table 3   0° inclination model face cycle pressure step

Push distance (m)	42	52	67	80	Average
Pressure step (m)	12	10	15	13	12.5

increased. As the inclination angle increases, the width difference increases as well.

Due to the increase of the dip angle, under the sliding effect, the fallen rock layer in the goaf is free to slide and fill. At the same time, it is restrained by the hinged beam, thus reducing the distance between the pressure arch and the working surface, so allowing sufficient time for the gas migration channel to be developed. In general, it is observed that the range of gas migration channels increases with the increase of the inclination angle.

Discussion

Formation and spatial distribution of pressure-relief gas migration channels

Through physical similarity simulation experiments, it is found that the crack distributions of overlying strata in the inclined coal seams are quite different from those in horizontal coal seams after being stressed in 2 to 3 cycles. In the fractured zones, more broken and separated cracks are interlinked (Sun et al. 2018). The overall shape of the fissures which is called an external ellipsoid produced by the overlying strata can be seen as the external boundary of the synthetic halves of the two halves' one. With the continuous advancement of the working face, the boundary morphology of the mining-induced fracture compaction zone of overburden rock forms two half-ellipsoid planes, which are called inner ellipsoid planes. Its internal and external boundaries spatially constitute the fissure-like ellipsoid zone of mining overburden rock (Shuang 2017). As the work surface continues to advance, the outer ellipsoid touches the main key stratum and stops developing in the vertical direction, while the inner ellipsoidal surface is continuously approaching the ellipsoidal surface in the vertical direction, due to the falling rock layers in the inclined coal seam. As a result, the elevations of the ellipsoidal projections do not develop upward in the end, and the gas migration channel for pressure-relief gas migration develops gradually in the process.

Through the simulation of two-dimensional physical similarity experiment and the mathematical model of the mining

Table 4   15° inclination model face cycle pressure step

Push distance (m)	35	45	52	70	85	Average
Pressure step (m)	8	10	7	18	15	11.6

Table 5   30° inclination model face cycle pressure step

Push distance (m)	45	55	65	75	90	98	Average
Pressure step (m)	10	10	10	10	15	8	10.5

fracture ellipsoid band, the mathematical models of the gas migration channel in the overlying strata under different coal seam inclination angles are established from Eqs. 1–5:

$$\begin{cases} \dfrac{(2x-Lb)^2}{Lb^2} + \dfrac{4y^2}{La^2} = \dfrac{z-mF1}{KC1mF1} \\[2mm] \dfrac{\left(2Lby-La\sqrt{Lb^2-(A1-A2)^2}-LbB1+LaLb\right)^2}{\left(La\sqrt{Lb^2-(A1-A2)^2}-LbB1+LbB2\right)^2} + \dfrac{(2x-Lb-A1+A2)^2}{(Lb-A1-A2)^2} \\[2mm] \hspace{6cm} = \dfrac{z-mF2}{KC2mF2} \end{cases} \quad (1)$$

$$Lb = \frac{h3}{\sin\theta} \tag{2}$$

$$\begin{cases} F1 = p1\mathrm{In}m + q1 \\ F2 = v1\mathrm{In}m + w1 \end{cases} \tag{3}$$

$$Fi = \frac{hi}{m} \tag{4}$$

Based on the elliptical band, an elliptical-like model of the dip coal seam is constructed. From Eqs. 1, 2, 3, and 4, Eq. 5 can be derived, which is the mathematical control model of the gas migration channel under different dip angles.

$$\begin{cases} \left(\dfrac{2\sin\theta x}{h_3}\right)^2 - \dfrac{4\sin\theta}{h_3} + 1 + \dfrac{(y-c)^2}{(La-c)^2} = \dfrac{h1-z}{h1c1} \\[3mm] \dfrac{\left(x-\dfrac{h_3}{2\sin\theta}+\dfrac{A_1-A_2}{2}\right)^2}{\left(\dfrac{h_3}{2\sin\theta}-\left(\dfrac{A_1+A_2}{2}\right)\right)^2} + \dfrac{(y-c)^2}{(c-B1)^2} = \dfrac{h2-z}{h2c2} \end{cases} \tag{5}$$
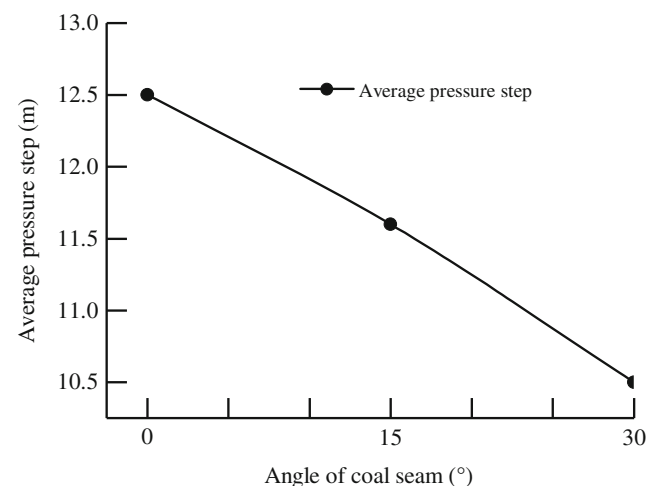

Fig. 3 Average pressure step distance of dip angles of different coal seams

where, L_a is the width of the working face (m); L_b is the advancing distance of the working face (m); h_1 is the height of the inner boundary of the gas migration channel (m); h_2 is the height of the gas boundary of the gas migration channel (m); K_{c1} and K_{c2} are the fracture and expansion coefficients of rock formations surrounded by the inner and outer boundaries of the gas migration channel. c is the distance between h_1, h_2 and inlet air slot (m); A_1 and A_2 are open cut, and the width of the dominant pass in the goaf above the working face (m); B_1 and B_2 are the widths of the dominant passages at the working face and the return air passage (m); θ is the inclination of the coal seam; F_1 and F_2 are the ratios of the height of the inner and outer elliptical surfaces to the height of the mining under the influence of height; p, q, v, and w are the coefficients; h_3 is the difference between the horizontal and the working faces (m).

Segregation analysis

B_q (the thickness of the strata between adjacent strata) is selected to describe the development of the dominant channel when the divergent angle of the coal seam is different (Jin 2018). With the progress of the working face, the crack propagations can be seen in the three stages, and the amount of separations within the working face continues to increase.

As the dip angle of the coal seam increases, the fracture area near the working face gradually increases, and the cracks at the lower part of the goaf are gradually reduced and closed. Under the effect of the declining effect, the falling rock layers of the goaf freely slide, resulting in an increase in the destructive space near the working face of the goaf. At the same time, since the fallen rock formation forms an articulated beam at the location of its crack, it formed a certain constraint on the rock that had already fallen, and the overburden will exist in the form of a reversed-inclined masonry structure. The reversed-inclined masonry structure makes the fallen form of the mining overburden extremely complicated, and the thickness of the bed-separated layer was also increased. It was difficult to completely compact the overlying strata, resulting in the gradual enlargement of the fracture zone near the working face. However, the falling space was gradually filled by the middle and upper fallen rock layers, which limits the collapse of the overlying strata in the lower gob, issue in a smaller extent of the overlying fissures, and the amount of bed separation was relatively small in the migration channel. Hence, a progressively larger gas migration channel near the working face forms such an asymmetric collapse pattern, as shown in Fig. 6.

Figure 6 shows abrupt changes in the amount of stratification near the dotted line. This is due to the influence of stress concentration on the side of the coal pillar and the gob side due to the effect of dip angle during the progress of the working face. The overlying strata are gradually compacted, and the amount of segregations decreases dramatically. This mutation provides the conditions for the formation of the gas

migration channel, which can be used as the basis for judging the boundary of the gas migration channel of cracks in overburden rocks.

Through degree analysis

According to the cracking characteristics of the overburden strata in the overburden fracture zone, when a hard, thick rock layer bends and sinks into the goaf, but does not completely break apart, the fracture gap of the rock stratum does not provide space for the gas migration. In order to describe the degree of fracture of the rock and the strength of the gas migration capacity in the fractured rock, the fracture propagation is introduced (Huang et al. 2010). Due to the existence of rock formations with different fracture propagations, the following provides the judgment basis for determining the gas migration channel for the migration of stope gas:

$$D_i = \frac{a_i}{h_i} \qquad (6)$$

where D_i is the through degree of the fractured gap in the rock formation (group) of the ith layer; h_i is the thickness of the rock formation (group) (m); a_i is the length of the broken fracture gap in the layer thickness direction (m).

It can be seen from Fig. 7 that as the dip angle of the coal seam increases, the fracture continuously propagates. When the working face begins to recover, the vertical displacement of the top rock layer of the working face increases with the increase of the inclination angle. At the same time, the stress of the overlying strata changes gradually from two-way compression to three-way pressure, increasing the tilting of strata and fracture propagations. Figure 7b combines the characteristics of the change in the degree of propagations between the rock formations in the fractured channel, providing a room for pressure-relief gas storage and transport.

Fractal dimension analysis

The study shows that the fracture distribution of overlying strata has good fractal characteristics (Amadu and Pegg 2018). In order to better analyze the change of the cracks in the paper, the fractured zones formed by the evolution process of the cracks in the gas migration channels are divided into several zones, and the fractal dimension of each zone of the gas migration channels under different coal seam inclination angles is analyzed. Generally, regular pattern analysis such as circles and squares is used to study the fractal law of images. The covered area is divided into squares of infinite length r, and the number of crack-containing squares is denoted as $N(r)$. When $r \to 0$, the slope of the double logarithm curve of $N(r)$ and r are the area to be studied. The fractal dimension value D, namely:
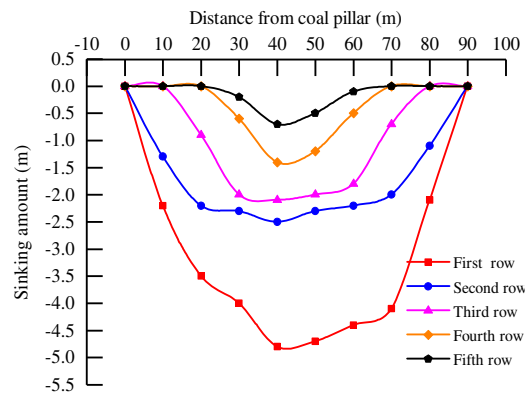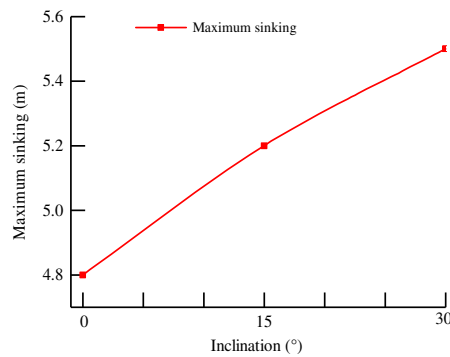
(a) 0° model first row line measurement point sinking amount
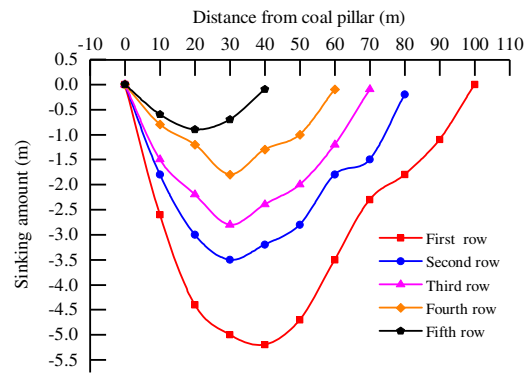
(b) 15° model first row line measurement point sinking amount
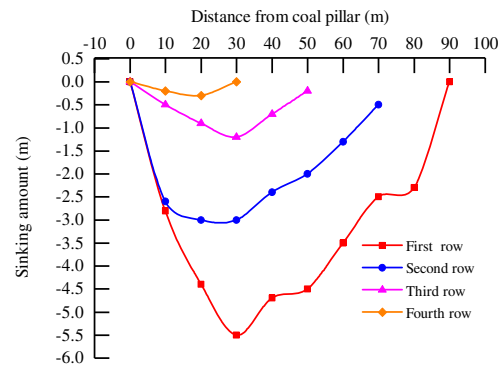
(c) 30° model first row line measurement point sinking amount

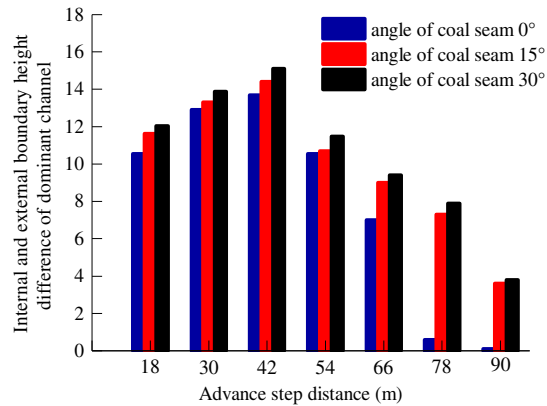(d) Relationship between dip angle and maximum subsidence

◀ **Fig. 4** The curve of the subsidence of the first row of lines with different inclination angles. **a** 0° model first row line measurement point sinking amount. **b** 15° model first row line measurement point sinking amount. **c** 30° model first row line measurement point sinking amount. **d** Relationship between dip angle and maximum subsidence

$$D = \lim \frac{\lg N(r)}{-\lg r} \qquad (7)$$

where r is the length of the square to cover the fracture area; $N(r)$ is the number of squares containing the fracture; D is the calculated fractal dimension value. The influence of dip angles of different coal seams on the complexity of cracks in the gas migration channel is further studied.

Figure 8a–c show that the dip of the coal seam has a significant impact on the fractures and deterioration of the overlying rock strata in the direction of the inclined plane. The falling height of the fallen rock layer increases with the increase of the dip angle. As the slope degree of sliding rock layer increases, the collapsing of the rock layer increases. The more complex the distribution of fracture networks in the fallen rock layers, the larger the fractal dimension.

Fig. 6 Distribution curve of layer separation at different dips

The dip angle has a substantial influence on the fractal dimension of the mining overburden fracture and the evolution of the fracture networks. From Fig. 8d, it can be seen that the dip angle and the fractal dimension are correlated. The collapsed formations of inclined coal seams are also complex and the fractal dimension is relatively large. Because the inclined masonry structure is the main damage type of inclined coal seams, the range and manner of distribution of the

Fig. 5 The height and width of the gas migration channel

(a) Height difference between the inner and outer boundaries of the gas migration channel under different dip angles of coal seams
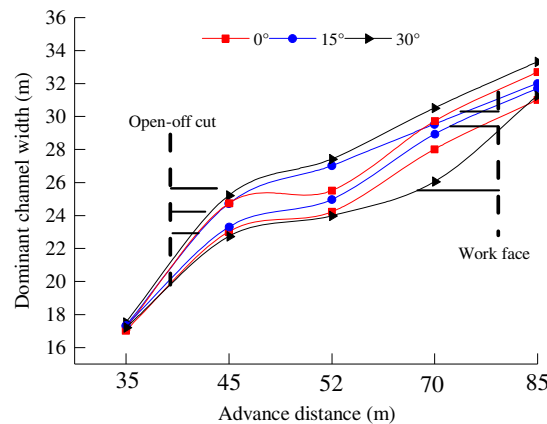
(b) Curve of gas migration channel width under different coal seam dip angles
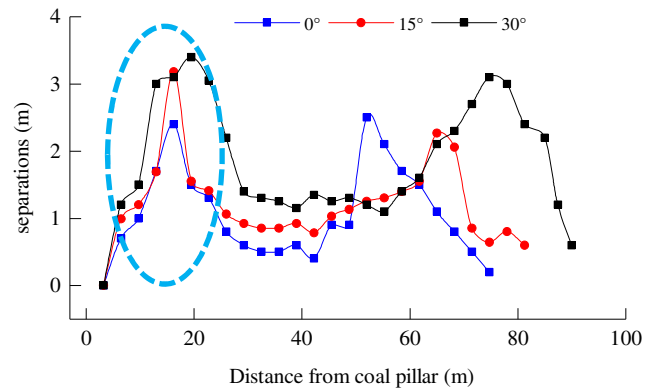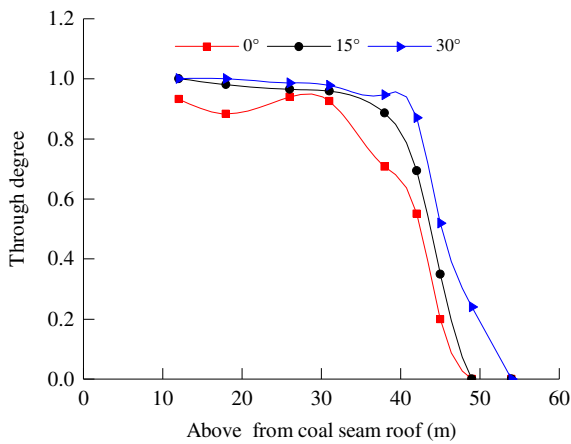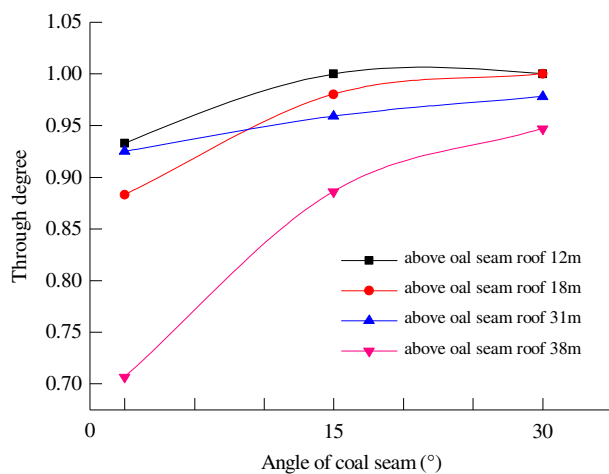
(a) Through degree of different dip angle channels

(b) Segmental penetration of different coal seam dip angle gas migration channels

Fig. 7 Curve of the penetration of gas migration channels at different coal seam inclination angles

overlying masonry structure have certain differences with the increase of coal seam inclination. The increase in the dip angle results in an increase in the height of the fallen space as well as an increase in the declining force of the falling rock strata in an oblique direction. These could lead to a more complete breakage of the collapsed strata in the inclined coal seam. As a result, the rock fractured, and the development of gas migration channels is getting progressed to provide better space for gas migration.

Field validation

High drill site layout and parameter settings

The test results show that the dip angle of coal seam substantially influences the development of gas migration

channel. By selecting the coal seam inclination angle, the arrangement of high-level boreholes field can be effectively determined. At the same time, it can guide the field to adopt the optimal drilling layout technology to carry out safe and efficient mining.

The wind tunnel and the return wind lane are excavated along the coal seam floor, and the eye is cut along the roof of the coal seam. The average coal seam inclination angle in Heshun is 7°. Based on the geometric condition, 10 boreholes are designed and constructed in the drilling site with two rows (Fig. 9).

The upper row of drill holes is 2.0 m away from the floor of the drilling floor, and the lower floor of the drill floor is 1.5 m. The first drill hole of the lower drill field is 0.4 m from the outside of the drill yard, and the rest of the drilling distance is 0.8 m.

Analysis of gas extraction effect of high-level borehole site

By observing the concentration of gas in a single hole of a drilling hole located at a high-level borehole field, the ratios of the gas extraction in the gas drilling field and the absolute gas emission volume in the wind discharge gas are obtained and shown in Fig. 10.
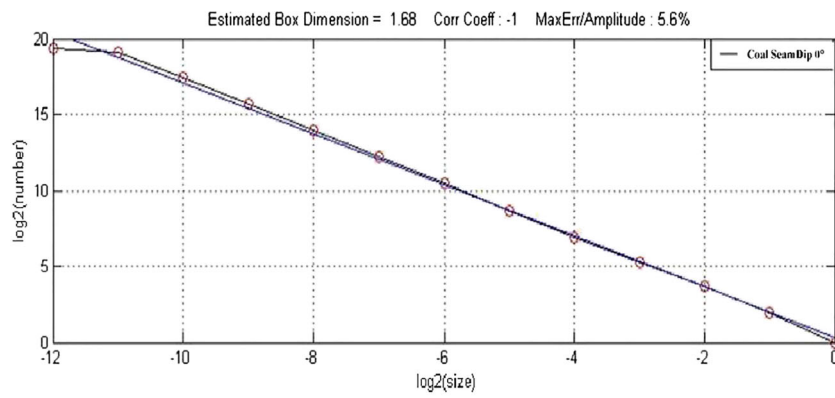
As can be seen in Fig. 10, in the normal mining process, the gas extraction volume of the high-level borehole site accounts for 49.94 to 89.88% of the total amount of absolute gas emission, and the volume of wind discharge gas accounts for 10.12~50.06% of the total gas emission of absolute gas.

### Gas extraction effect of high-level borehole site

Figure 11 shows the real-time observation of gas concentration in the upper gas corner and return airway. As can be seen in Fig. 11, the gas concentration changes in the upper corner and return airway demonstrate the effect of a high-elevation borehole in governing the gas extraction on the upper corner and return air volume. It is noticed that the average concentration of gas in the upper corner is maintained below 0.27% and the average concentration of gas in the return airway is maintained below 0.32% so as to ensure a safe and an efficient mining environment.
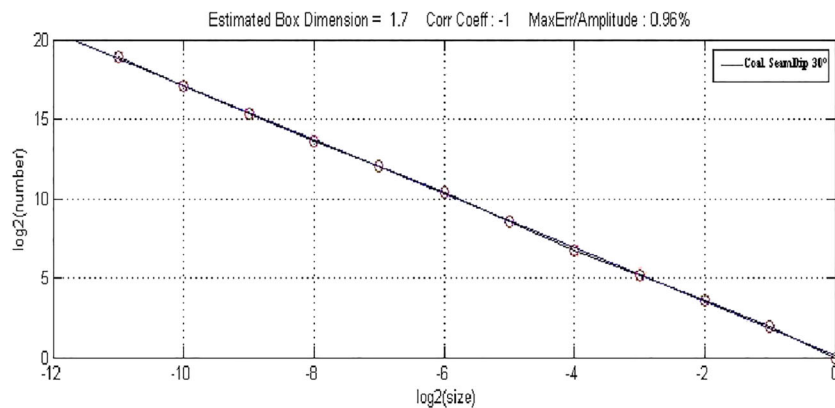
Conclusions

1. Through physical similarity simulation tests, the evolution of gas migration channels under different coal seam inclination angles was explored, and the space-time morphology model of mining gas migration channel was constructed. The increase in the dip angle of the coal seam results in an increase in the height of the three zones and

Estimated Box Dimension = 1.68 Corr Coeff : -1 MaxErr/Amplitude : 5.6%

(a) Fractal dimension of gas migration channel with an inclination of 0°

Estimated Box Dimension = 1.69 Corr Coeff : -1 MaxErr/Amplitude : 2%

(b) Fractal dimension of gas migration channel with an inclination of 15°

Estimated Box Dimension = 1.7 Corr Coeff : -1 MaxErr/Amplitude : 0.96%

(c) Fractal dimension of gas migration channel with an inclination of 30°
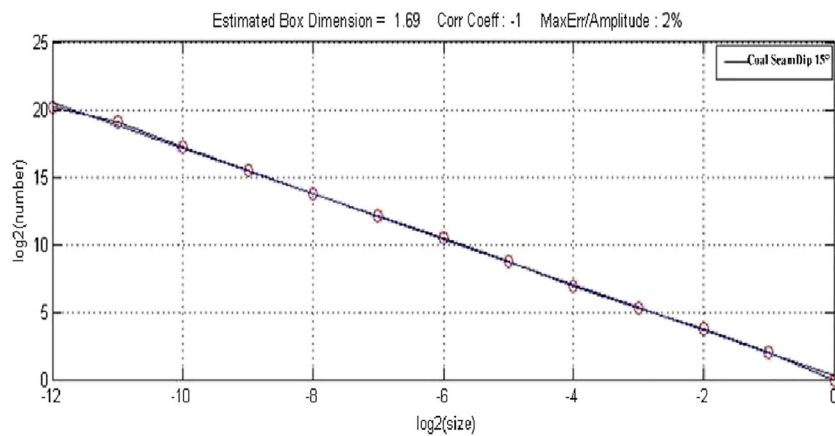
Fig. 8 The variation of fractal dimensions of gas migration channel in different coal seams. **a** Fractal dimension of gas migration channel with an inclination of 0°. **b** Fractal dimension of gas migration channel with an inclination of 15°. **c** Fractal dimension of gas migration channel with an inclination of 30°. **d** Fractal dimension fitting of gas migration channel with different dip angles

an increase in the mean pressure step width. The average pressure at zero inclination angle is 12.5 m, while the average pressures measured at inclination angles of 15° and 30° are 1.08 and 1.09 times greater than the original pressure (0°). The increase in the dip angle of the coal seam results in an increase in the developing height, width, and scope of the gas migration channel.

2. With the advancing of the working face, the fractures in the rock propagated gradually from bottom to top. As the advancing distance increases, the fracture distributions of the coal seams vary depending on the direction of dip angles. When a dip angle increased, the fractal dimensions of coal seams were measured in between 1.68, 1.69, and 1.71,

(4-5)04 Work face track slot
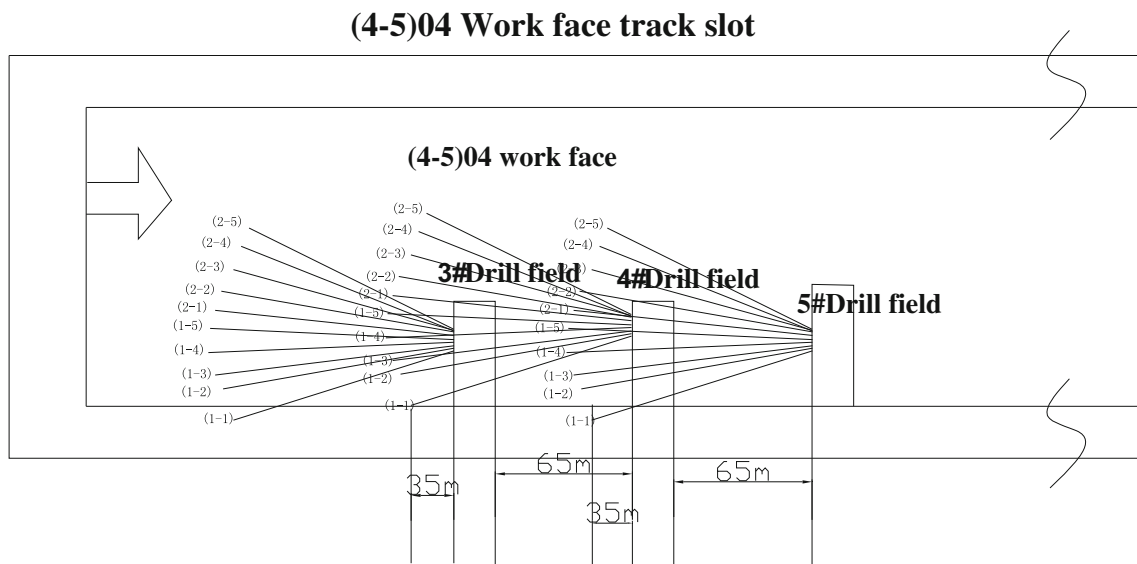
(a) High-level boreholes site drilling construction plan
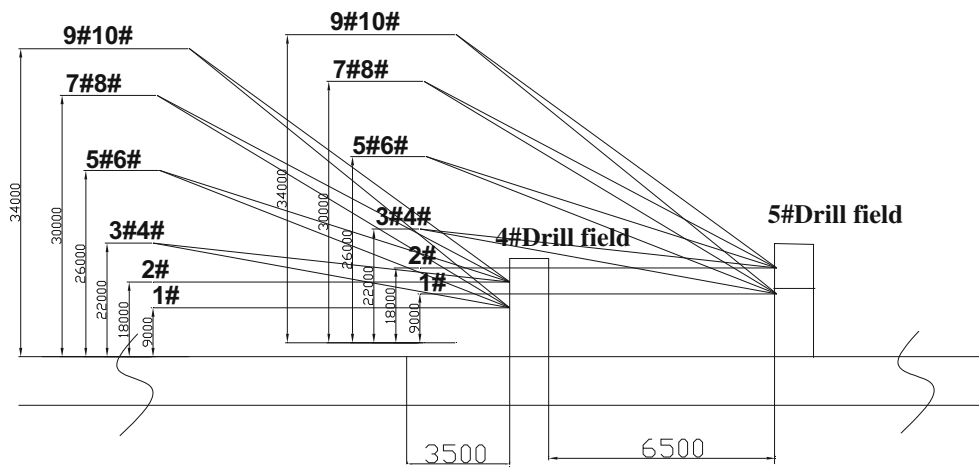
(b) High-level boreholes field drilling profile

Fig. 9 Layout of borehole in high-level borehole field. **a** High-level borehole site drilling construction plan. **b** High-level borehole field drilling profile

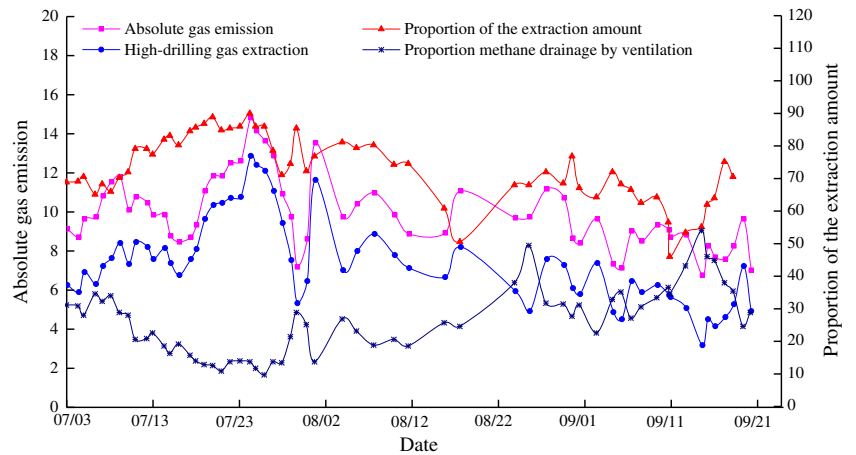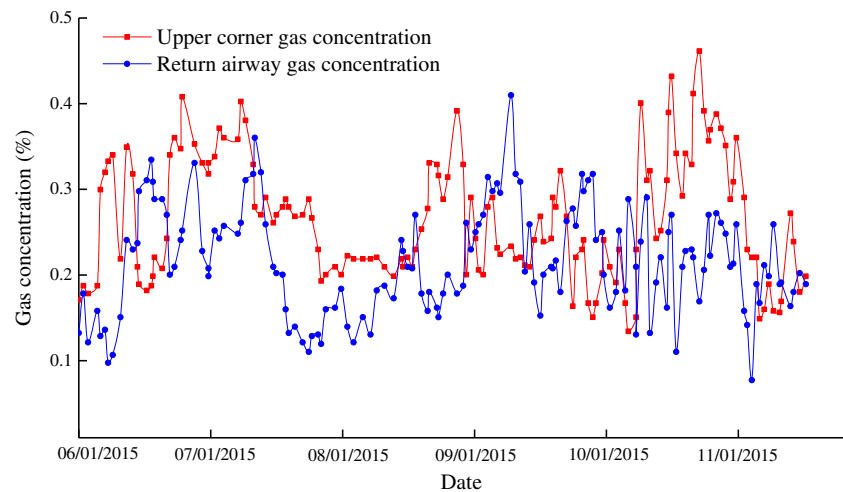**Fig. 10** Extraction effect of high-level borehole field

Fig. 11 Variation of gas concentrations at upper corner and return airway

displaying an increasing trend. The segregation rates and through degree of the gas migration channel were found to be proportional to the inclination of the coal seam.

3. A high-level borehole field was arranged according to the results of the physical similarity simulation tests, and the on-site gas extraction activity was monitored and analyzed. Gas extracted through this high-level borehole field reached from 49.94 to 89.88% of the absolute gas emission. The average concentration of gas in the upper corner was maintained below 0.27% and the average concentration of gas in the return airway was maintained below 0.32% so as to ensure a safe and an efficient mining environment.

References

Amadu M, Pegg MJ (2018) Theoretical and experimental determination of the fractal dimension and pore size distribution index of a porous sample using spontaneous imbibition dynamics theory. J Pet Sci Eng 167:785–795 [In English]

Do TN, Wu JH, Lin HM (2017) Investigation of sloped surface subsidence during inclined seam extraction in a jointed rock mass using discontinuous deformation analysis. Int J Geomech 17(8). [In English]):04017021

Gu HL, Tao M, Wang JX, Jiang HB, Li QY, Wang W (2018) Influence of water content on dynamic mechanical properties of coal. Geomech Eng 16(1):85–95 [In English]

Guo H, Yuan L (2015) An integrated approach to study of strata behave our and gas flow dynamics and its application. Int J Coal Sci Technol 2(1):12–21

Guo PF, Zhang XH, Jin ZP (2016) Analysis of the "semicircular arch" structure in deep inclined thick coal seam caving mining. Min Res Dev 36(11):6–11

Huang BX, Liu CY, Xu JL (2010) Overlying rock fracture through degree. J China Univ Min Technol 39(1):45–49

Jin K, Cheng YP, Ren T, Zhao W, Tu QY, Dong J, Wang ZY, Hu B (2018) Experimental investigation on the formation and transport mechanism of outburst coal-gas flow: implications for the role of gas desorption in the development stage of outburst. Int J Coal Geol 194:45–58 [In English]

Lai XP, Sun H, Shan PF, Cai M, Cao JT, Cui F (2015) Structure instability forecasting and analysis of giant rock pillars in steeply dipping thick coal seams. Int J Miner Metall Mater 22(12):1233–1244 [In English]

Li SG, Lin HF, Zhao PX (2014a) Dynamic evolution of mining fissure elliptic paraboloid zone and extraction coal and gas. J China Coal Soc 39(8):1455–1462

Li SG, Lin HF, Zhao PX (2014b) Mining fissure elliptic paraboloid zone and dynamic evolution of coal and methane mining. J China Coal Soc 39(8):1455–1462

Li SG, Ding Y, An ZF (2016) Experimental research on the shape and dynamic evolution of repeated mining-induced fractures in short-distance coal seams. J Min Saf Eng 33(05):904–910

Li SG, Shuang HQ, Wang HS, Kill S, Liu L (2017) Extraction of pressurized gas in low air-conductivity coal seam using drainage roadway. Sustainability 9(2):223–239

Li L, Qin BT, Ma D, Zhuo H, Liang HJ, Gao A (2018a) Unique spatial methane distribution caused by spontaneous coal combustion in coal mine goafs: an experimental study. Process Saf Environ Prot 116:199–207 [In English]

Li Z, Xu JL, Ju JF, Zhu WB, Xu JM (2018b) The effects of the rotational speed of voussoir beam structures formed by key strata on the ground pressure of stopes. Int J Rock Mech Min Sci 108:67–79 [In English]

Liu TQ (1995) Influence of mining activities on mine rock mass and control engineering. J China Coal Soc 20(1):1–5

Liu J, Chen SL, Wang HJ, Li YC, Geng XW (2015) The migration law of overlay rock and coal in deeply inclined coal seam with fully mechanized top coal caving. J Environ Biol 36(4):821–827 [In English]

Palchik V (2015) Bulking factors and extents of caved zones in weathered overburden of shallow abandoned underground workings. Int J Rock Mech Min Sci 79:227–240 [In English]

Pan RK, Cheng YP, Yuan L, Yu MG, Dong J (2014) Effect of bedding structural diversity of coal on permeability evolution and gas disasters control with coal mining. Nat Hazards 73(2):531–546 [In English]

Qian MG, Miao XX (1996) Research on the key strata theory in ground control. J China Coal Soc 21(3):225–230

Shan PF, Lai XP (2018) Numerical simulation of the fluid-solid coupling process during the failure of a fractured coal-rock mass based on the regional geostress. Transp Porous Media 124(3):1061–1079 [In English]

Shuang HQ (2017) Evolving mechanism and application of advantage passage for pressure relief gas storage and transportation in mining of slowly inclined coal seam. Xi'an University of Science and Technology

Sun J, Wang LG, Zhao GM (2018) Failure characteristics and confined permeability of an inclined coal seam floor in fluid-solid coupling. Adv Civ Eng [In English]

Wang HW, Wu YP, Cao PP (2015) Large-scale, three-dimensional, loadable, similar simulation tests for coal mining with large dip angles. J China Coal Soc 40(7):1505–1511

Wang HW, Wu YP, Xie PS (2018) Mining thickness effect of coal wall stability in long-wall large mining face with large angle coal seam. J Min Saf Eng 35(1):64–70

Wu JY, Feng MM, Xu JM, Qiu PT, Wang YM, Han GS (2018a) Particle size distribution of cemented rockfill effects on strata stability in filling mining. Minerals 8(9) [In English]

Wu QS, Jiang LS, Wu QL, Xue YC, Gong B (2018b) A study on the law of overlying strata migration and separation space evolution under hard and thick strata in underground coal mining by similar simulation. Dyna 93(2):175–181 [In English]

Xie HP, Ju Y, Gao F, Gao MZ, Zhang R (2017) Groundbreaking theoretical and technical conceptualization of fluidized mining of deep underground solid mineral resources. Tunn Undergr Space Technol 67:68–70 [In English]

Xue S, Yuan L, Wang YC, Xie J (2014) Numerical analyses of the major parameters affecting the initiation of outbursts of coal and gas. Rock Mech Rock Eng 47(4):1505–1510 [In English]

Yuan L (2016) Strategic thinking on CO mining of coal and gas in China. J Coal Soc 41(1):1–6

Yuan L (2017) Scientific concept of coal precision mining. J China Coal Soc 42(1):1–7

Zhang YJ, Gao C (2016) Failure characteristics of overlying strata in fully mechanized top-coal caving mining with horizontal slicing in steeply inclined and thick coal seam. Coal Sci Technol 44(1):126–132

Zhang Y, Zhang B, Liu JK (2013) Mechanism of destruction and slippage in deep inclined thick coal seam to long-wall mining. Coal Sci Technol 41(10):9–12

Zhang XL, Cheng YP, Wang L, Zhao W (2015) Research on the controlling effects of a layered sill with different thicknesses on the underlying coal seam gas occurrence. J Nat Gas Sci Eng 22:406–414 [In English]

Zhang CL, Xu J, Peng SJ, Li QX, Yan FZ, Chen YX (2018a) Dynamic behavior of gas pressure and optimization of borehole length in stress relaxation zone during coalbed methane production. Fuel 233:816–824 [In English]

Zhang C, Zhang L, Zhao YX, Wang W (2018b) Experimental study of stress permeability behavior of single persistent fractured coal samples in the fractured zone. J Geophys Eng 15(5). [In English]):2159–2170